

~ 1 eV are pulled out of the trap through the space between the trap electrodes. This threshold was measured empirically with a mixture of noble gases as a test sample. In the secular scanning mode the potential depth for the masses of interest was adjusted to be about 6 eV. The secular excitation field was then applied only to the center section of the trap (see Fig. 3) in order to eject ions mainly when they were close to the detector.

The entire beam generation, collision and storage apparatus is located in a single 30 cm diameter ultra-high vacuum (UHV) chamber. A 150 l s^{-1} turbo pump evacuates the system to a background pressure of 10^{-10} mbar. This vacuum is advantageous for both long storage times and for the generation of pure ionic particle beams. A gas filling system permits operation with a buffer gas background, typically helium, at a pressure of $P \approx 5 \times 10^{-6}$ mbar. In this way it is possible to quickly cool the trapped ions to nearly room temperature. The cooling has a noticeable effect in improving the mass resolution of the trap spectrometry [30,31], due to the small initial energy spread of the cooled ions. For Mg^+ ions, laser cooling has also been successfully employed to reach the mK temperatures regime, demonstrating this as an alternative cooling technique for trapped atomic ions with spectrally narrow, optically accessible resonances. For molecular ions, sympathetic laser cooling is also a possible method for achieving similarly low sample temperatures [17].

Two networked personal computers are employed with this experimental system. The master computer is used to control the overall operation of the apparatus in order to repeatably load ionic samples into the trap, and to record the relevant experimental parameters, whereas the slave computer is solely tasked with collecting data from the PMT or the EMT. A careful sequence of oven preheat, ion loading, collisional cooling, analyse and pause times (see Fig. 6) is required to achieve well defined ion samples and repeatable collision conditions within the trap.

4. Experimental results and discussion

4.1. Mass spectrometry and mass-selective purification

Q-scan mass spectrometry was utilized to generate low resolution mass spectra covering large mass regions. Fig. 7 displays examples of such measurements with either a mixture of various noble gases or assorted ionic states of C_{60} loaded into the trap. An entire spectrum could be generated in one second and covered a mass/charge range in excess of two orders of magnitude. Experimentally, this is accomplished by scanning the trapping field amplitude down to zero. The sacrifice accepted in generating these large mass range spectra in a short time is that of poor resolution. The maximum observed resolution ($m/\Delta m$ or $z/\Delta z$) was between 5 and 6 and was relatively mass independent over large mass ranges within the experimental domain of 20–1000 u. An advantage of this technique is that the positioning of the strongly biased EMT just outside the electrodes results in a very high collection efficiency. In this geometry the masses are actually pulled out of the trap by the EMT biasing field, with relatively few ions striking the electrodes as they leave the trapping volume.

The data in Fig. 7 demonstrate both the strengths and weaknesses of the simple theoretical model proposed for this system. Calibration of the abscissa (mass axis) of Fig. 7(a) employed the predicted quadratic dependence of the mass on the rf-field amplitude U_{rf} . This figure shows that this model holds well for a single charge state, and further measurements have shown that a single mass calibration can hold over a range of masses as large as 20–800 u. However, it appears that the same does not hold true for samples with differing charge states. Although Eq. (8) suggests that the charge state of a q-scan ejected ion should have an inverse quadratic dependence on U_{rf} , experimental measurements with multiply charged fullerenes indicated that different charges were ejected with a $U_{\text{rf}}^{-1.38}$

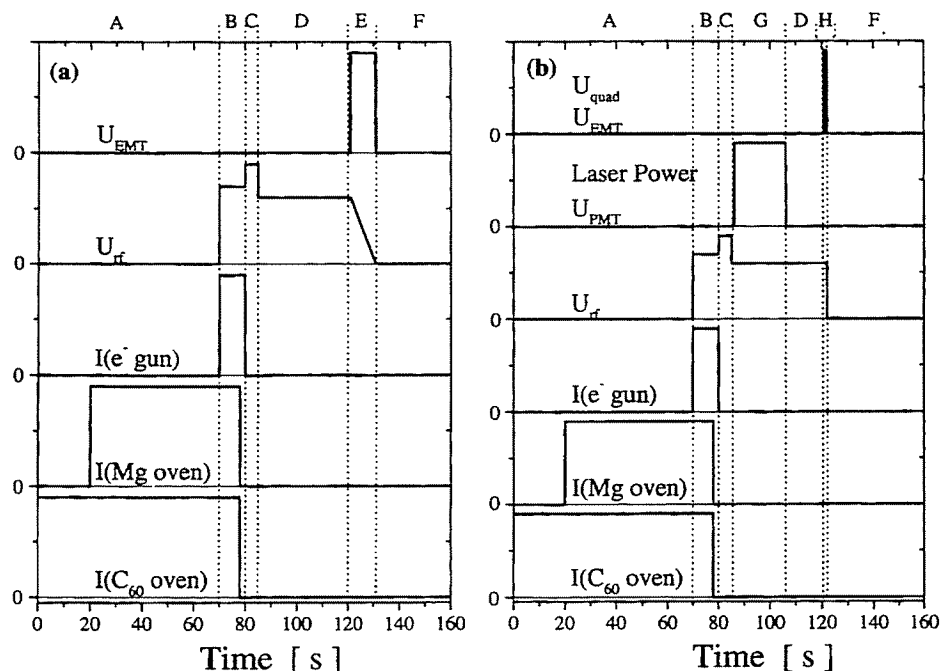


Fig. 6. Timing diagrams for controlling the ovens, electron beams, trap parameters, laser exposure and detection electronics for both (a) q-scan and (b) secular scan/laser photodissociation experiments. The temporal components of the experiment, as indicated in the figure, are: A: oven heating, B: trap loading, C: low mass removal and buffer gas cooling, D: buffer gas cooling, E: q-scan mass spectrum collection, F: inter-experiment wait time, G: laser exposure, and H: secular scan mass spectrum collection.

dependence. At present, we do not completely understand this empirically determined exponent, probably because the present model is too simplified to describe the process perfectly.

Figs 8 and 9 demonstrate mass spectra generated by secular excitation of mass-selected ions out of the trap. These scans took approximately 5–10 s to cover a mass range of 150 u by scanning the frequency of the quadrupole field driving the secular excitation. With this technique, only a limited range of masses can be analysed in one scan, since the detection efficiency depends on the mass. However, the mass range is easy to change by simply readjusting the experimental parameters between scans. This inconvenience is more than compensated for by the high resolution that is possible with this technique. Fig. 8 shows an $m/\Delta m$ resolution of approximately 800 near 130 u. The resolution is mass dependent and drops off to about 250 at

720 u (Fig. 9). This resolution was demonstrated for a simple experimental geometry, and obvious improvements should make even higher values achievable (see ref. [32] for a high resolution $\omega_{\text{exc}} = \omega_{\text{sec}}$ technique). The collection efficiency with this technique is over an order of magnitude lower than the q-scan technique. This lower efficiency results from the expulsion of many of the ions directly into the trap electrodes rather than towards the EMT. Both the mass and charge dependences of the excitation field given in Eq. (9) were confirmed experimentally.

Mass resolution and collection efficiency are rather sensitively dependent on the selection of the parameters of the driving field, i.e. amplitude and scan rate. The physical reason for this is the dynamic response of a trapped ion to the driving field. The ion can gain energy only at a certain rate, and it must build up the energy in order to escape from the trap. Therefore, there is an

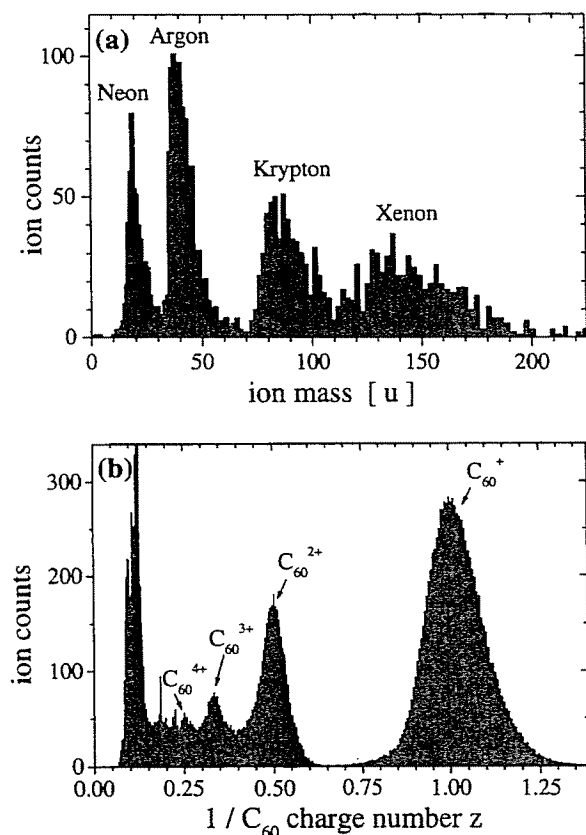


Fig. 7. Mass spectra generated in the linear ion trap using the q-scan technique. Plot (a) shows a single scan of a mixed sample of neon, argon, krypton and xenon ions while plot (b) shows the spectra generated by averaging 10 scans of samples containing several charge species of fullerene molecules. Only the first four charge states of C_{60} are observable due to the resolution limits of the system. The abscissa calibrations were based on $m \propto U_{rf}^2$ and $z \propto U_{rf}^{-1.38}$ for plots (a) and (b), respectively. At low mass, unresolved peaks of background ions are present.

optimum for the secular scan field amplitude and frequency scan rate and for the trapping potential depth. For example, if the driving field amplitude is too low the collection efficiency drops off sharply, while too high an amplitude can adversely effect the resolution. Typical parameters used in our work were secular scan amplitudes of 1 V_{pp} , scan rates of 200 kHz s^{-1} , and trapping potential depths of about 6 eV . Under these conditions the driving field is only a small perturbation compared to the rf trapping field. For maximum resolution, a small number

of ions should be cooled to near room temperature by viscous collisions in helium before scanning.

As mentioned in Section 2.2, the mass selective techniques have also been used to purify trapped samples. By increasing the trapping rf amplitude, the trap can be used as a high-pass filter by removing low masses as their q -values exceed 0.908 (Eq. (7)). This technique was used to efficiently remove Mg^+ from samples of collisionally generated MgC_{60}^+ . Reducing the trap amplitude could be used to operate the trap as a low-pass filter as the large mass ions can be pulled out of the trap when their trapping depth becomes too low (q -scanning). Given a reasonably large mass separation, either one of these techniques can be used to give basically 100% purification with almost no loss of the ions of interest. If the desired result is to selectively remove ions of a mass which is close to the mass to be studied (e.g. remove C_{60}^+ while keeping MgC_{60}^+), then secular excitation is the best approach due to its high resolution. However, for such close masses it has only been possible to achieve about a 10 to 1 improvement when small losses at the desired masses were required. It appears that collisional heating of the wanted masses or collective heating of the entire ion cloud may be limiting the efficiency of this technique. The best approach we have utilized so far is to scan the excitation frequency back and forth over a small mass range around the unwanted mass with parameters similar to those used for secular scans.

4.2. Collision reaction measurements

The experimental arrangement for typical ion–molecule collision experiments is shown in Fig. 2(c). A small molecular oven is positioned collinear with the trap axis at one end of the trap. The diffusive beam of molecules generated by this oven is densest at that end of the trap within the trapping volume. The ion source described in Section 3 is positioned at the opposite end of the

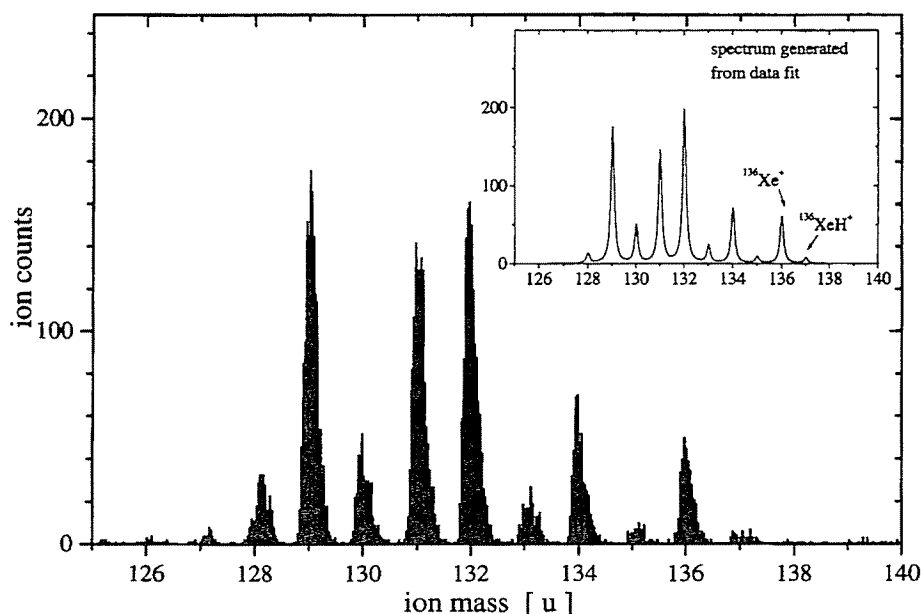


Fig. 8. Secular scan mass spectrum of a sample of Xe^+ ions with a resolution of $m/\Delta m \approx 800$, showing the presence of the major naturally occurring isotopes. A spectral fit based on the known natural abundances of xenon (inset) demonstrates a mass-insensitive detection efficiency over this limited range of masses. The main fitting parameter was the fraction of XeH^+ present in the trapped sample (11%).

trap. The molecular end of the trap has its potential lowered relative to the ion end, to accelerate the ions to kinetic energies of up to about 200 eV before they interact with the

molecules. During the collision process several types of reactions have been observed including complex formation, charge transfer, and molecular fragmentation. In general, a helium buffer gas

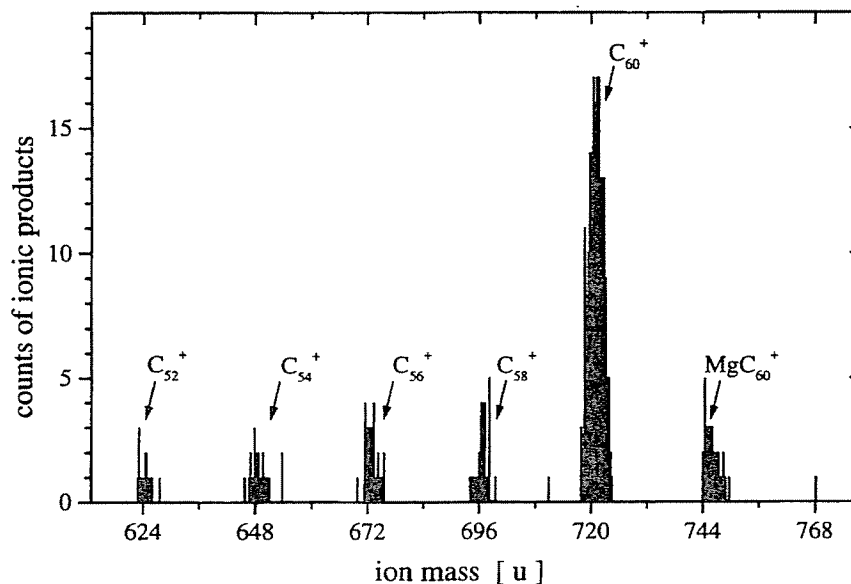


Fig. 9. A mass spectrum of the products resulting from controlled energy collisions between Mg^+ and C_{60} . The collision energy was 60 eV and the products from fragmentation, charge exchange and complex-formation reactions are indicated.

at a pressure of roughly 5×10^{-6} mbar is used to remove much of the energy which was transferred in the collisions into the internal degrees of freedom of the products, before analysis is carried out. For a small cloud of ions, this reduces the temperature of the vibrational and rotational population distributions to close to room temperature. The trap is set to collect almost all of the reaction products, so that mass spectrometry can be used to quantify the results (see Fig. 9).

In order to maximize control over the collision energy involved in the reactions, it is necessary to avoid trapping the reactant ions for times long enough to lose significant energy through scattering off of trapped ions, neutral molecules, buffer gas atoms, or background particles. Therefore, the trapping field amplitude is modulated in order to periodically destabilize the mass of the injected ions above and below the storage threshold given by Eq. (7) (Fig. 10). A typical frequency for this modulation was 5 kHz, with the amplitude of the modulation selected so that the ions were stable for about 2/3 of the time. In this manner, the average lifetime is of the order of the time necessary for an ion to pass the length of the trap, which means that ions which do not react with the molecular cloud fall out of the trap. In our experiments, the higher mass reaction products were unaffected by this modulation. In this way it is possible to collect energy resolved collision reaction data of the type shown in Fig. 11. The drawback of this approach is that only a small fraction of the incident ions produce collision reactions, and the yields of the product ions are low. Naturally, this modulation technique is only applicable for the investigation of reaction products of sufficiently high mass relative to the injected ions.

In an alternative approach, the reactant ions are not removed periodically from the trap and their density increases with time, resulting in a strongly increasing rate of collisions. The advantage of this approach is an improvement of up to four orders of magnitude in the generation of product ions. However, the energy resolution of

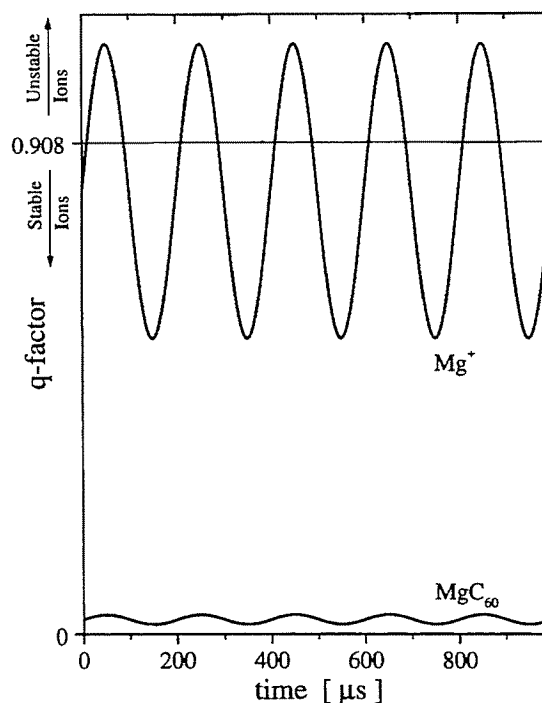


Fig. 10. Plots of the time dependence of the q -factors for Mg^+ and MgC_{60}^+ ions during the amplitude modulation of the trapping field which is used to reduce the lifetime of the Mg^+ reactant ions in the trap during energy-resolved collision reactions. The line at $q = 0.908$ indicates the stability threshold of the trap.

the measurement is lost and the ability to work at high collision energies is limited by the possibility of collisional destruction through fragmentation of the product ions held in the trap by the large number of high energy reactant ions also held in the trap. One other aspect of this technique is that the reactant ion densities can be increased such that multibody collision processes can be observed.

Several different types of collision studies have already been carried out with this apparatus and the details will be published elsewhere [19,21]. The following gives a brief compilation, with the goal of demonstrating the capabilities of the system rather than discussing the details of the physical processes themselves. Fig. 9 shows a demonstration of the types of reaction which are observable in the trap. Neutral C_{60} molecules are impacted by accelerated Mg^+ ions. The mass

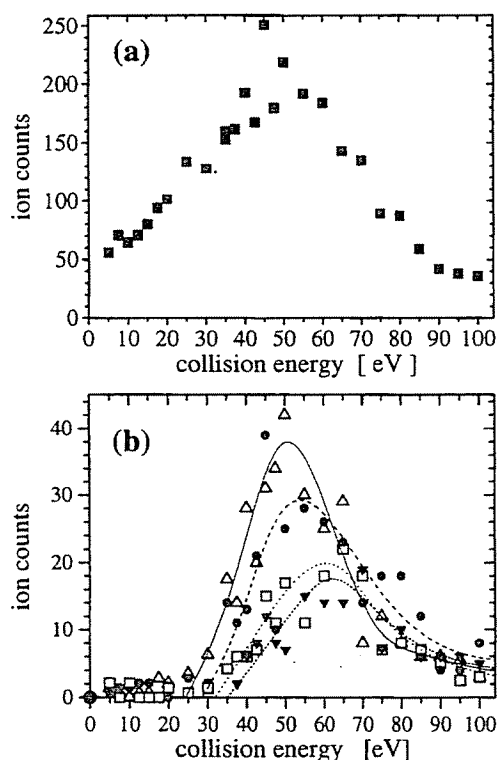


Fig. 11. Demonstration of energy-resolved data using collision reactions between C_{60} and Mg^+ . The plots show the number of product ions formed by (a) charge transfer reactions producing C_{60}^+ ions (\blacksquare) and (b) fragmentation reactions producing C_{58}^+ ions (Δ), C_{56}^+ ions (\bullet), C_{54}^+ ions (\square) and C_{52}^+ ions (\blacktriangledown). The broad peak in the C_{60}^+ curve demonstrates the effect of a Massey resonance [33] in the charge transfer reaction [19,21]. The reaction times were 20 s for all measurements.

spectrum demonstrates the presence of MgC_{60}^+ from complex formation reactions, C_{60}^+ from charge transfer reactions, and C_{58}^+ , C_{56}^+ , C_{54}^+ etc. molecules formed by fragmentation. All of these reactions have been observed as a function of collision energy (e.g. Fig. 11).

Another type of collision study exploits the storage feature of an ion trap. It is possible to perform collision experiments at very low reactant-ion kinetic energies such as $E < 100$ meV. Such an experiment consists of first loading the trap with reactant ions, cooling the ions to near room temperature (buffer gas cooling) or below (laser cooling), and then interacting the cold ions with neutral reactants. Data near 0 eV for colli-

sions between Mg^+ and C_{60} have been obtained with this technique [19,21], and an example is shown in Fig. 11(b).

Finally, electron beams passing through the center of the trap have been used for electron impact studies such as single and multiple ionization and fragmentation of fullerene molecules. Results from this type of experiment are compiled in Fig. 12.

4.3. Optical spectroscopy

Two optical spectroscopic techniques have been demonstrated with this apparatus: resonance fluorescence and molecular photofragmentation. The techniques are not exclusive and in fact can be employed simultaneously, with the results often yielding complementary information.

The observation of laser-induced fluorescence (LIF) is a sensitive technique for the detection and analysis of trapped ions with a strong electric dipole transition. In fact, samples as small as a single ion have been observed [34,35]. In principle, the most effective approach for detecting LIF in a linear trap is to probe collinearly with the trap axis to permit the largest overlap between the trapped ion cloud and the laser beam. With the present set-up the positioning of the ion source and molecular oven prevent axial illumination. Instead, the probe beam travels at a 15° angle to the trap axis and probes only the central region of the trapping volume. Nevertheless, LIF from atomic ions is still observable and has been carried out using stored Mg^+ ions (Fig. 14, inset). In principle, LIF spectroscopy of trapped molecular ions is possible, although to date the only molecules which have been loaded into the trap are fullerenes, whose gas-phase visible spectrum is expected to be very weak, with only solid and solution phase spectra known at present (e.g. [36]).

Laser photodissociation (LPD) studies have recently been carried out with MgC_{60}^+ complexes [18,20]. In these experiments, the trap is loaded

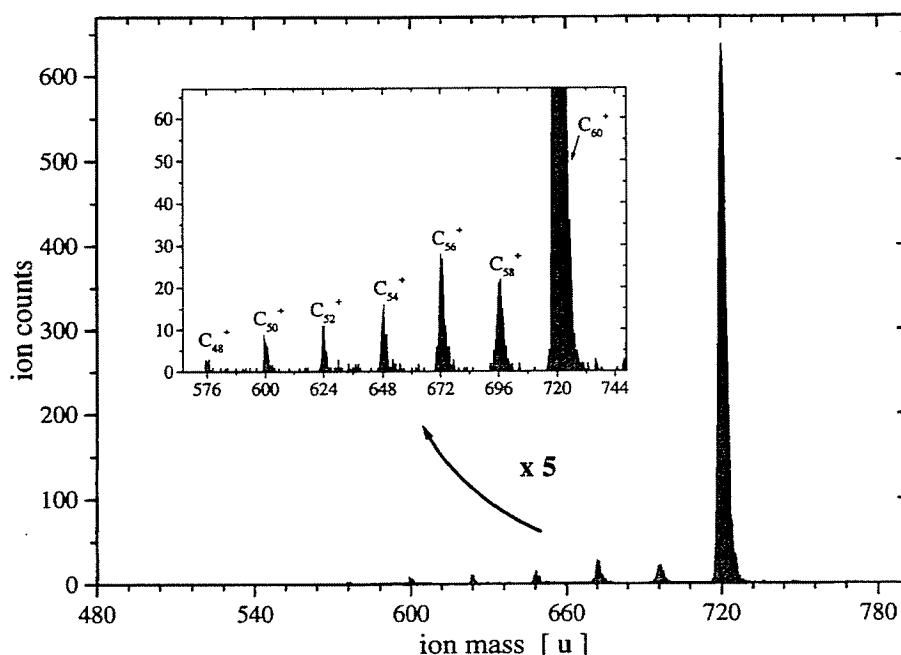


Fig. 12. An ion trap secular scan mass spectrum of electron impact ionization of C₆₀ fullerenes, demonstrating fragmentation as well as charge-transfer reactions. Similar curves were observed for the doubly charged ionic products.

with collisionally generated fullerene complexes and then exposed to dissociating laser radiation (see Fig. 5). We have two techniques for studying the photodissociation processes which have proven to be complementary in practice.

The first technique is widely applicable to a large variety of molecules. It is a direct mass spectrometric measurement of LPD made by examining the mass distribution of the samples after various laser exposures. These measurements yield the photodissociation rate of the compound of interest. A computer is employed to repeatedly load the trap with equivalent molecular samples. After each loading the trap is exposed to laser radiation for a chosen period of time. In general, four different periods are selected, with the trap content being measured after each. The number of undissociated ions is plotted semi-logarithmically as a function of time. In the case of the fullerene complexes, the MgC₆₀⁺ count is plotted versus time and an exponential fit yields the rate constant for photodissociation (Fig. 13). Since the necessary parameters

of the trapped sample and of the laser beam are known, it is possible to convert the rate constant directly to the absolute, total, photodissociation cross-section [18,20]. Measurement of the photodissociation cross-section as a function of photon energy can provide useful information on the molecular potential energy surfaces. One of the interesting features of this approach is that the long trapped lifetime of the ions permits the measurement of extremely slow reaction rates. Using exposure times of 0.5, 2, 4 and 6 s we have measured rates below 0.2 s⁻¹. Much longer exposure times are in principle possible and would permit the determination of even slower rates. A related point is that the ability to measure exceedingly slow rates permits the use of very low cw-laser intensities such as, typically, below 100 W cm⁻². This in turn results in measurements of pure first-order reaction processes with no interference from multiphoton effects.

In addition to measuring total cross-sections, the present technique can also be utilized for the

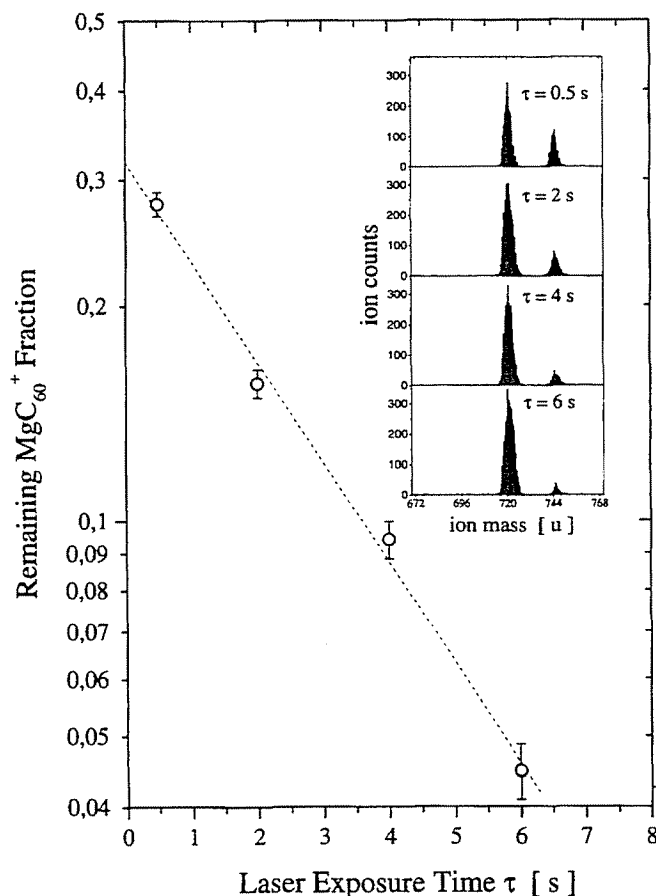


Fig. 13. A semilogarithmic plot of reactant ion number vs laser exposure, demonstrating a measurement of the linear photodissociation rate of MgC_{60}^+ when exposed to 10 mW of $\lambda = 591.6$ nm radiation. The inset displays the mass spectrometric data used to generate the main plot.

measurement of photodissociation branching ratios. In the case of MgC_{60}^+ , we have determined that the complex dissociates into either $\text{Mg}^+ + \text{C}_{60}$ or $\text{Mg} + \text{C}_{60}^+$. By simultaneously measuring the destruction of MgC_{60}^+ and the production of C_{60}^+ , it was possible to determine the branching ratio for this reaction [20]. For accurate measurements care must be taken to avoid loading too many ions into the trap, which can result in the loss of the fragment ions after photodissociation.

The complementary technique for the determination of absolute photodissociation cross-sections is LIF measurements of LPD. This approach is less generally applicable as it requires reactions where a product ion has a

strong LIF transition. However, it is a complementary and fast approach to the same measurement. Rather than monitoring the destruction of the reactant molecule, this technique monitors the generation of a product such as Mg^+ in $\text{MgC}_{60}^+ \rightarrow \text{Mg}^+ + \text{C}_{60}$. This pump-probe approach requires two lasers, one to photodissociate the sample, and the second to probe for the appearance of the dissociation products. By monitoring the LIF as a function of time, a $(1 - e^{-Rt})$ curve is observed (Fig. 14) which yields the reaction rate and thus the cross-section. This is done with a single loading of the trap rather than the multiple loading of the mass spectrometric approach. In order to measure slow reaction rates, good stability of the wavelength

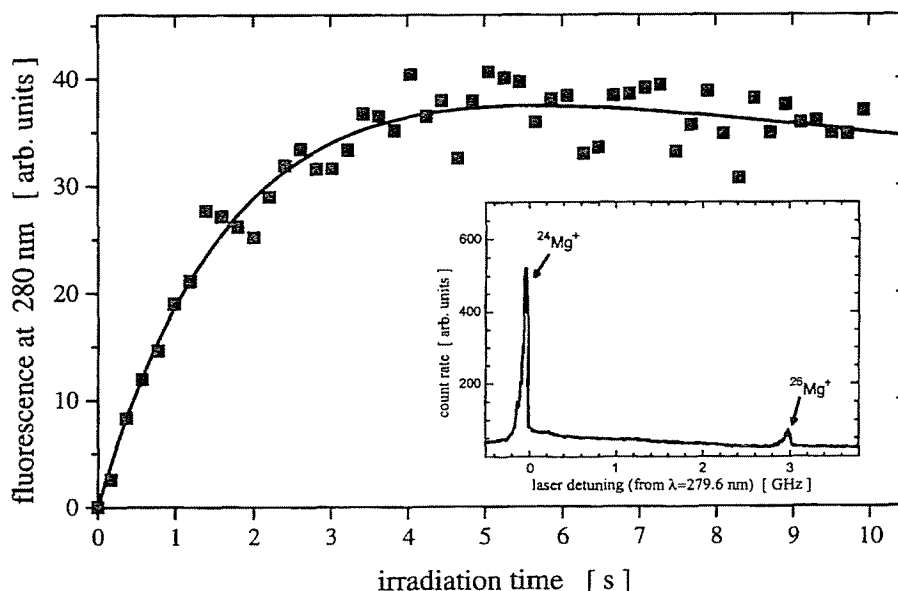


Fig. 14. Plot of the 280 nm fluorescence as a function of time from Mg^+ ions created by photodissociation of MgC_{60}^+ during exposure to 10.5 mW of $\lambda = 560$ nm radiation. The squares are the experimental data points without any averaging, and the solid line is an $e^{at}(1 - e^{-Rt})$ fit which yields the total dissociation rate, R . The insert shows the laser-induced fluorescence spectrum of trapped Mg^+ . Two isotopic peaks separated by about 3 GHz can be seen in the spectrum.

and intensity of the probe laser is required. In addition, one must minimize any photodissociation by the probe laser by using low laser intensities, and by chopping the probe laser beam.

Finally, it should be noted that similar techniques should be equally applicable for laser photoionization measurements.

5. Conclusions

A compact experimental system for the generation, storage, purification and analysis of gaseous ionic complexes has been developed. The system can handle atomic and molecular ions as well as ionic complexes. Precise, mass-dependent, purification of the samples is possible, and the apparatus has been used to study both unimolecular (photodissociation, photoionization) and bimolecular (collisional) reactions. Control over most of the reaction conditions is possible. In our apparatus it

includes the application of collision energies of up to 200 eV, and the use of buffer gas cooling and/or laser cooling to reach low reaction temperatures. In addition, the reactant ion and neutral densities and buffer gas pressures during the reaction process can be controlled. Analysis of the reactants and products is carried out with both mass spectrometric and laser spectroscopic techniques. Both low resolution, wide mass range, and high resolution mass spectrometric analysis is possible. The former relies on the manipulation of the q -parameters of the trapped ions, and the latter results from exciting the secular ion motion by parametric excitation. In addition, laser-induced fluorescence and absolute and partial photodissociation cross-section measurements have been carried out. The particular feature of studying ion-molecule complexes in their vibrationally and rotationally relaxed state has been carried out for the first time and is expected to find ongoing applications.

Acknowledgements

The authors would like to express their thanks to Dr J. Wanner for the many helpful discussions in which he participated.

References

- [1] D. Gerlach, *Physica Scripta* T59 (1995) 256.
- [2] Z. Wan, J.F. Christian, Y. Basir, S.L. Anderson, *J. Chem. Phys.* 99 (1993) 5858.
- [3] A.B. Raksit, D.K. Bohme, *Int. J. Mass Spectrom. Ion Processes* 55 (1983) 69.
- [4] G.H. Dunn, *Physica Scripta* T59 (1995) 249.
- [5] F.M. Penning, *Physica* (Amsterdam) 3 (1936) 873.
- [6] P. Boissel, P. Marty, A. Klotz, P. de Parseval, B. Chaudret, G. Serra, *Chem. Phys. Lett.* 242 (1995) 157.
- [7] W. Paul, O. Osberghaus, E. Fischer, Ein Ionenkafg, *Forschungsberichte des Wirtschafts- und Verkehrsministeriums Nordrhein-Westfalen*, 415, 1958.
- [8] E. Fischer, *Z. Physik* 156 (1959) 1.
- [9] M.A. Armitage, J.E. Fulford, D.-N. Hoa, R.J. Hughes, R.E. March, *Can. J. Chem.* 57 (1979) 2108.
- [10] N. Zhang, Y. Matsuo, M. Takami, *Chem. Phys. Lett.* 244 (1995) 133.
- [11] W. Paul, M. Raether, *Z. Phys.* 140 (1955) 262.
- [12] J.L. Elkind, F.D. Weiss, J.M. Alford, R.T. Laaksonen, R.E. Smalley, *J. Chem. Phys.* 88 (1988) 5215.
- [13] R.T. McIver, R.L. Hunter, G. Baykut, *Rev. Sci. Instr.* 60 (1988) 400.
- [14] C. Berg, T. Schindler, G. Niedner-Schattenburg, V.E. Bondybey, *J. Chem. Phys.* 102 (1995) 4870.
- [15] S.M. Michael, M. Chien, D.M. Lubman, *Rev. Sci. Instrum.* 63 (1992) 4277.
- [16] T.L. Grebner, H.J. Neusser, *Intern. J. Mass Spectrom. Ion Processes* 137 (1994) L1.
- [17] T. Baba, I. Waki, *Jpn. J. Appl. Phys. Pt 2 — Lett.* 35 (1996) L1134.
- [18] M. Welling, R.I. Thompson, H. Walther, *Chem. Phys. Lett.* 253 (1996) 37.
- [19] M. Welling, H.A. Schuessler, R.I. Thompson, H. Walther, in K.M. Kadish and R.S. Ruoff (Eds.), *Recent Advances in the Chemistry and Physics of Fullerenes and Related Materials*, Vol. 4, PV 97–14, The Electrochemical Society Proceeding Series, Pennington, NJ, 1997, p. 751.
- [20] R.I. Thompson, M. Welling, H. Walther, in K.M. Kadish, R.S. Ruoff (Eds.), *Recent Advances in the Chemistry and Physics of Fullerenes and Related Materials*, Vol. 4, PV 97–14, The Electrochemical Society Proceeding Series, Pennington, NJ, 1997, p. 70.
- [21] R.I. Thompson, M. Welling, H.A. Schuessler, H. Walther (to be published).
- [22] W. Paul, *Angew. Chem. (Int. Ed., English)* 29 (1990) 739.
- [23] W. Paul, in E. Arimondo, W. D. Phillips, F. Strumia (Eds.), *Laser Manipulation of Atoms and Ions*, Proc. International School of Physics 'Enrico Fermi', Course CXVIII, 9–19 July 1991, North-Holland, Amsterdam, 1992, p. 497.
- [24] H.G. Dehmelt, in D.R. Bates, I. Esterman (Eds.), *Advances in Atomic and Molecular Physics*, Vol. 3. Academic Press, New York, 1967, p. 53.
- [25] R. Bluemel, C. Kappler, W. Quint, H. Walther, *Phys. Rev. A* 40 (1989) 808.
- [26] G. Rettigshaus, *Z. Angew. Phys.* 22 (1967) 321.
- [27] J.E. Fulford, D.-N. Hoa, R.J. Hughes, R.E. March, R.F. Bonner, G.J. Wong, *J. Vac. Sci. Technol.* 17 (1980) 829.
- [28] L.D. Landau, E.M. Lifshitz, *Mechanics*, Vol. 1, Sect. 27, Pergamon Press, Oxford, 1976.
- [29] D.R. Dennison, *J. Vac. Sci. Technol.* 8 (1971) 266.
- [30] R.E. March, R.J. Houghes, in J.D. Wineforder (Ed.), *Quadrupole Storage Mass Spectrometry*, Chemical Analysis, Vol. 102, John Wiley & Sons, New York, 1989.
- [31] O. Chun-Sing, H.A. Schuessler, *Int. J. Mass Spectrom. Ion Phys.* 35 (1980) 305.
- [32] F.A. Londry, R.E. March, *Int. J. Mass Spectrom. Ion Processes* 144 (1995) 87.
- [33] R.E. Johnson, *Introduction to Atomic and Molecular Collisions*, Plenum Press, New York, 1982, p. 136.
- [34] F. Diedrich, E. Peik, J.M. Chen, W. Quint, H. Walther, *Phys. Rev. Lett.* 59 (1987) 2931.
- [35] E. Peik, G. Hollemann, H. Walther, *Phys. Rev. A* 49 (1994) 402.
- [36] K. Kikuchi, S. Suzuki, Y. Nakao, N. Nakahara, T. Wakabayashi, H. Shiromaru, K. Saito, I. Ikemoto, Y. Achiba, *Chem. Phys. Lett.* 216 (1993) 67.

Webster's
Third
New International
Dictionary
OF THE ENGLISH LANGUAGE
UNABRIDGED

A Merriam-Webster
REG. U.S. PAT. OFF.

*Utilizing all the experience and resources of more than
one hundred years of Merriam-Webster® dictionaries*

EDITOR IN CHIEF
PHILIP BABCOCK GOVE, Ph.D.
AND
THE MERRIAM-WEBSTER
EDITORIAL STAFF



MERRIAM-WEBSTER INC., *Publishers*
SPRINGFIELD, MASSACHUSETTS, U.S.A.



A GENUINE MERRIAM-WEBSTER

The name *Webster* alone is no guarantee of excellence. It is used by a number of publishers and may serve mainly to mislead an unwary buyer.

A *Merriam-Webster*® is the registered trademark you should look for when you consider the purchase of dictionaries or other fine reference books. It carries the reputation of a company that has been publishing since 1831 and is your assurance of quality and authority.

COPYRIGHT © 1986 BY MERRIAM-WEBSTER INC.

PHILIPPINES COPYRIGHT 1986 BY MERRIAM-WEBSTER INC.

WEBSTER'S THIRD NEW INTERNATIONAL DICTIONARY
PRINCIPAL COPYRIGHT 1961

Library of Congress Cataloging in Publication Data
Main entry under title:

Webster's third new international dictionary of
the English language, unabridged.

Includes index.

1. English language—Dictionaries. I. Gove,
Philip Babcock, 1902-1972. II. Merriam-Webster Inc.
PE1625.W36 1986 423 85-31018
ISBN 0-87779-201-1 (blue Saurite)
ISBN 0-87779-206-2 (imperial buckram)

All rights reserved. No part of this work covered by the copyrights hereon may be reproduced or copied in any form or by any means—graphic, electronic, or mechanical, including photocopying, recording, taping, or information storage and retrieval systems—without written permission of the publisher.

MADE IN THE UNITED STATES OF AMERICA

41K88

ELECTROSPRAY IONIZATION MASS SPECTROMETRY

**FUNDAMENTALS, INSTRUMENTATION,
AND APPLICATIONS**

Edited by

Richard B. Cole

Department of Chemistry, University of New Orleans, New Orleans, Louisiana



A WILEY-INTERSCIENCE PUBLICATION

JOHN WILEY & SONS, INC.

New York • Chichester • Weinheim • Brisbane • Singapore • Toronto

This text is printed on acid-free paper.

Copyright © 1997 by John Wiley & Sons, Inc.

All rights reserved. Published simultaneously in Canada.

Reproduction or translation of any part of this work beyond that permitted by Section 107 or 108 of the 1976 United States Copyright Act without the permission of the copyright owner is unlawful. Requests for permission or further information should be addressed to the Permissions Department, John Wiley & Sons, Inc., 605 Third Avenue, New York, NY 10158-0012.

Library of Congress Cataloging in Publication Data:

Electrospray ionization mass spectrometry : fundamentals, instrumentation, and applications / edited by Richard B. Cole.

p. cm.

"A Wiley-Interscience publication."

Includes index.

ISBN 0-471-14564-5 (cloth : alk. paper)

1. Mass spectrometry. 2. Ionization. 3. Biomolecules--Analysis.

I. Cole, Richard B., 1956- .

QP519.9.M3E44 1997

574.19'285--dc20

Printed in the United States of America

10 9 8 7 6 5 4

CHAPTER 3**ESI Source Design and Dynamic Range Considerations**

ANDRIES P. BRUINS

University Centre for Pharmacy, Groningen, The Netherlands

Abstract	107
I. Electrospray nebulization	108
II. Electrospray construction and operation	110
A. High-voltage connection	110
B. Electrospray and electrical discharge	114
C. Flow rate and sensitivity	115
D. Position of the sprayer inside the source	116
III. Atmospheric pressure ionization source construction	118
A. Free jet expansion into vacuum	118
B. Cluster ion formation	120
1. Prevention	120
2. Curing	122
C. Focusing of ions at atmospheric pressure	122
D. Vacuum system design	122
E. Vacuum system and sensitivity	124
F. Ion-sampling orifice	126
G. Ion optics between sampling orifice and mass analyzer	129
IV. Up-front collision-induced dissociation	130
V. Mass-scale calibration	132
VI. Dynamic range in electrospray	133
References	135

ABSTRACT

Mass spectrometer ion sources are normally located inside a high-vacuum envelope. An ion source operating at atmospheric pressure is better suited, if not essential, for a growing number of applications. Highly polar, thermolabile, and

Electrospray Ionization Mass Spectrometry, Edited by Richard B. Cole.
ISBN 0-471-14564-5 © 1997 John Wiley & Sons, Inc.

ionic samples and biopolymers require the application of electrospray ionization (ESI) at atmospheric pressure. Electrospray ionization source design is a combination of charged-aerosol generation techniques for ion formation and atmospheric pressure source and associated vacuum technology for mass separation and detection. Limitations inherent in simple ES have been removed in mechanically assisted ESs. Vacuum-system design and ion optics are of decisive importance for sensitivity and reliability. Collision-induced dissociation just outside the source is inherent in atmospheric-pressure sources. It is easy to use, effective, and comes at no cost. Limited dynamic range at the high sample concentration end is a fundamental problem in ES. Dynamic range extension by different source design is not within reach using presently available technology.

I. ELECTROSPRAY NEBULIZATION

The nebulization of liquids by electrical forces is carried out on a very small scale in the recently developed microelectrospray accessory for mass spectrometry, and on a grand scale in the electrostatic spray painting of automobiles and the electrostatic spray deposition of pesticides on crops (1). Electrospray is the dispersion of a liquid into electrically charged droplets, and as such combines two processes: droplet formation and droplet charging. The formation of small, micron-sized droplets does not present a problem if the liquid flow rate, surface tension, and electrolyte concentration are low. An increase of one or more of these variables makes it more difficult for the electric field to produce the desired charged aerosol for mass spectrometry. The electric field strength at the sprayer tip can be increased to try and overcome the adverse effects of the aforementioned three variables, an electric field that is too high will give rise to an electrical discharge that accompanies the ES process. A discharge can be tolerated in some spray applications, but is detrimental in ESMS. Electrical discharge is particularly troublesome in the formation of negatively charged droplets.

Modifications to the simple ES system, as shown in Figure 1, are aimed at increasing the tolerance toward adverse effects of high liquid-flow rate, surface tension, and electrolyte concentration. Dilution of an aqueous solution with an organic solvent reduces surface tension. Coaxial addition of a sheath flow of methanol, acetonitrile, ethanol, isopropanol, or 2-methoxyethanol to the sample solution at the tip of the spray capillary was first used for the combination of capillary electrophoresis with ESMS and later also used for sample infusion and LC coupling with ESMS (2,3). In sheath-flow-assisted ES, the electric field alone has to disperse *and* charge the liquid in one operation.

In industrial applications of ES, the input of mechanical energy is used for the dispersion of liquids at high flow rates. Droplet charging is done by exposing the mechanical sprayer to a high electric field. For example, a rotating disk combined with an electric field created by a 100-kV power supply may be used in spray painting.

The assistance of a high-velocity gas flow or mechanical vibration is used in

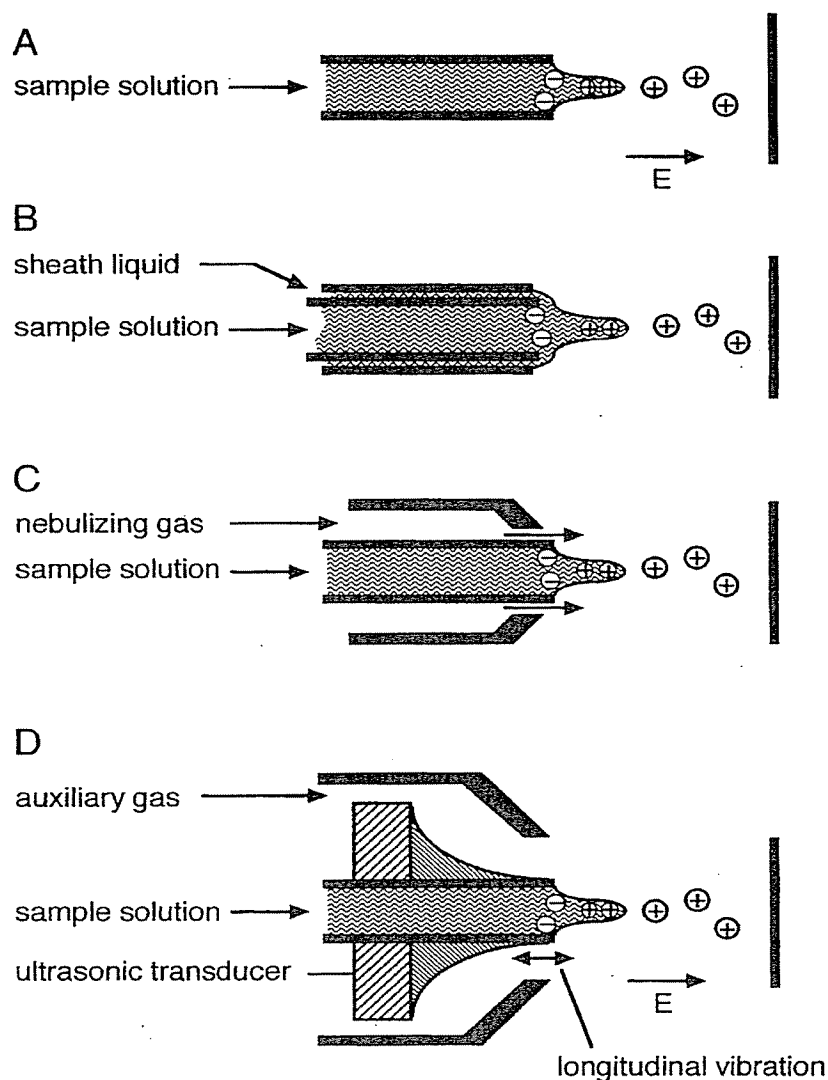


Figure 1. Aerosol formation by ES. (a) Simple ES; (b) ES with sheath flow; (c) ES with pneumatic assistance; (d) ES with ultrasonic assistance.

ESMS (4–6). In a simple approximation, the pneumatic or ultrasonic nebulizer takes care of aerosol formation, while the electric field does the droplet charging. When compared with “pure” ES, pneumatically assisted ES can handle aqueous solutions and higher flow rates without the need for critical adjustment and can be operated at a lower field strength so that electrical discharge is eliminated. Ultrasonic assistance offers the same advantages, but is a more complex and more expensive combination of mechanical and electronic devices. The trade names of some such devices are IonSpray (SCIEX) and Ultraspray (Analytica of Branford).

Charged droplets generated by ES spread out in a wide angle. A moderately fast coaxial gas flow can be used to try and keep the droplets in a narrower beam. Such pneumatic focusing can be combined with a coaxial sheath flow (3,7) and

with ultrasonic nebulization (6). The focusing gas flow is not intended for pneumatic nebulization. Pneumatic focusing increases the number of ions transported into the vacuum envelope of the mass spectrometer. Pneumatically assisted ES produces a narrow beam of droplets by the very nature of the high-velocity gas flow used in the concentric nebulizer. High-flow ES in Finnigan instruments makes use of pneumatic nebulization and a separate auxiliary (focusing) gas flow that prevents wetting of the nebulizer by redeposition of droplets on the outside of the sprayer.

Pneumatically and ultrasonically assisted ES can work at liquid flow rates up to a few hundred microliters per minute. Pure, unassisted ES can be extended to very low flow rates. Microelectrospray has the advantage of extremely efficient use of a sample solution: one microliter can produce ions for about 40 min, long enough for performing a number of MS/MS experiments. A very low flow rate microsprayer is compatible with the electroosmotic flow in a capillary electrophoresis column, eliminating the need for a make-up flow.

A regular ES device is constructed from approximately 0.3 mm o.d., 0.1 mm i.d. stainless-steel tubing, or a coaxial arrangement of fused silica and stainless-steel capillaries. Stability at low flow in a microsprayer requires a miniaturized version having narrower inside and outside diameter. A 10- to 50- μm i.d. fused-silica capillary is tapered on the outside by etching with hydrofluoric acid (8) or by mechanical abrasion (9). Electrical contact with the liquid stream is made by the application of silver paint (8), or by deposition of gold (9). Making contact at the tip is necessary for CE/MS (8,9). For sample introduction from a loop injector or from a syringe pump, it is sufficient to make electrical contact upstream from the tip by clamping the narrow-bore, fused-silica capillary in a metal union (10,11). Caprioli and co-workers have prepared an integrated microcolumn/microsprayer with the aim of online concentration of dilute samples (11). Wilm and Mann have constructed a microsprayer for the analysis of small volumes of peptide solutions at a flow rate of about 25 nL/min (12). A 1-mm o.d., 0.6-mm i.d. glass capillary is pulled out to an inside diameter of 1–3 μm by means of an electrode puller. The outside of the capillary is coated with gold. Approximately 1 μL of a sample solution is loaded into the capillary, and gas pressure is applied to push the liquid toward the tip.

II. ELECTROSPRAY CONSTRUCTION AND OPERATION

A. High-Voltage Connection

The tip of an ES capillary is exposed to a high electric field. In principle, the field can be generated by connecting the sprayer to a high-voltage supply and the source to ground, by grounding the sprayer and connecting the source to high voltage, and by connecting both the sprayer and the source to separate power supplies set to different voltages. Selection of either of these options depends on the mass analyzer and the system chosen for the transportation of ions from the

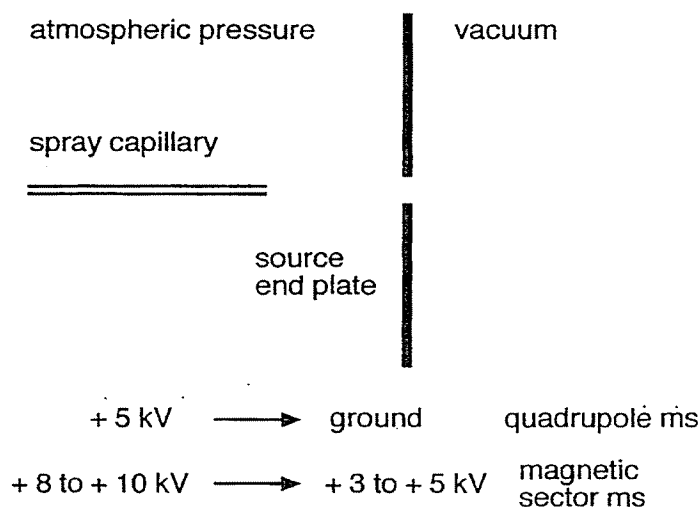


Figure 2. Voltage arrangements for ES capillary and source; no isolation between source end plate and MS accelerating voltage.

atmospheric-pressure source region into the vacuum of the mass analyzer. In a quadrupole mass spectrometer, the ion source can be at ground potential and the sprayer at up to plus or minus 5 kV (4,13). In most magnetic-sector mass spectrometers the accelerating voltage is limited to 3–5 kV during ES operation, so that the voltage on the sprayer is 8–10 kV with respect to ground (see Fig. 2).

Safety is not a major problem, since the source can be designed for protection of the operator by the use of appropriate insulation and safety interlocks. If the sprayer is at high voltage, the connection to the HPLC or infusion pump can be made from fused-silica capillary tubing. One should keep in mind that a fused-silica capillary filled with an electrolyte solution is not an insulator but a resistor, which may conduct enough to give the operator an itch if the needle or plunger of a syringe in an infusion pump is touched during ES operation. For safety reasons, one should not make or break a connection between syringe and transfer line when the ES high voltage is on. As a further safety measure, the needle of the syringe in an infusion pump can be connected to ground.

Of more practical value is the question of whether high voltage on the sprayer interferes with operation of a capillary electrophoresis system, and whether the high voltage has an influence on the transportation of a sample through the fused-silica transfer line.

Let us first consider capillary electrophoresis. Off-line CE experiments are usually conducted by applying 30 kV between anode and cathode. In CE/MS with positive ion operation, the anode is at 30 kV, while the cathode is at the high voltage of the ES interface, for example, at 5 kV. The voltage drop over the column is reduced to 25 kV, resulting in longer analysis time.

There are more electrical implications to CE/MS other than just the voltage drop over the CE column. In Figure 3A the simplest CE/MS system is drawn schematically. Current flowing from the CE power supply is carried away only to

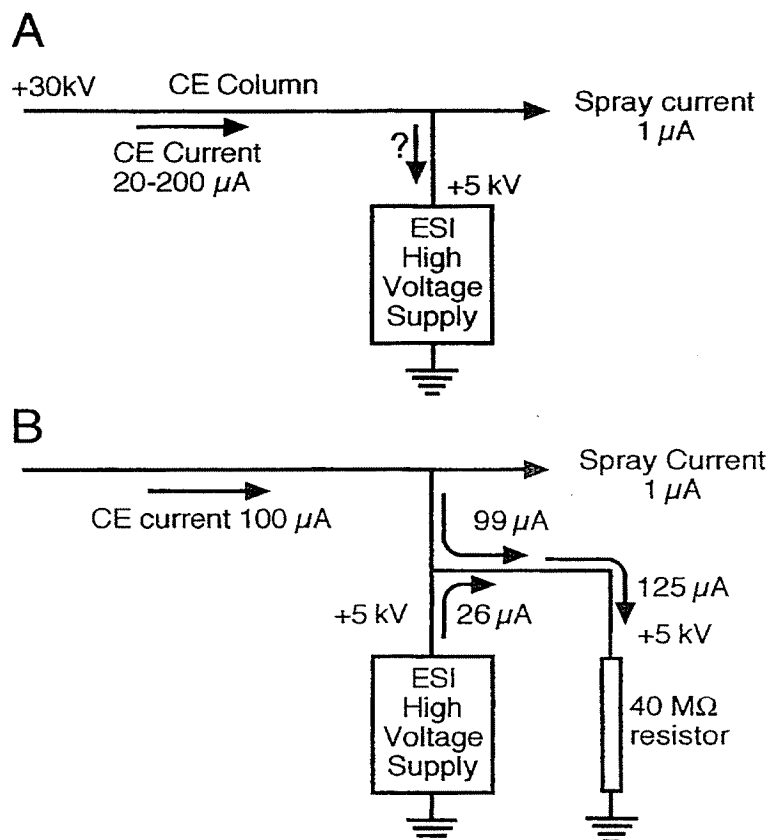


Figure 3. (A) Currents flowing in a simple CE/MS system using a CE high-voltage supply and an ES high-voltage supply; CE current, 100 μA ; charge transportation on droplets, 1 μA ; ES power supply has to sink 99 μA . (B): 40-M Ω load resistor connected between ES supply and ground carries 125 μA at 5 kV (Ohm's law); ES power supply has to deliver 26 μA to maintain current balance.

a minute extent as charge on sprayed droplets. Most of the current has to flow into the ES power supply, which has been designed to *supply* current, not to *sink* current. If the supply has to sink too much current, its internal feedback circuit, which stabilizes the output voltage to a preset value, cannot keep the power supply under control, resulting in an uncontrolled rise of output voltage and unstable ES. By connecting an additional load resistor, as shown in Figure 3B, the power supply is forced to deliver current, and output stability is maintained. The user should consult the high-voltage power supply specifications for selection of the correct resistance value. Of course these CE/MS current considerations do not apply if the spray capillary is at ground.

Less obvious and often overlooked is the possibility of electromigration in the transfer line between the electrosprayer and a syringe pump used for sample infusion. To conserve sample, the liquid flow rate may be reduced to 1 $\mu\text{L}/\text{min}$, corresponding to a linear velocity of 50 cm/min in a 50- μm i.d. capillary or 12 cm/min in a 100- μm i.d. capillary. If a positively charged sample molecule has a

mobility of $10^{-3} \text{ cm}^2/\text{Vs}$ and if a 50-cm long transfer capillary is used with 5 kV on the electrosprayer, the electrophoretic velocity of the sample is 6 cm/min in the direction from the sprayer back into the syringe. In this example, there should be no problem if a 50- μm i.d. transfer capillary is used: the liquid velocity far exceeds the opposing electrophoretic velocity. A 100- μm i.d. capillary (liquid velocity 12 cm/min at 1 $\mu\text{L}/\text{min}$) can still be used at 5 kV. The situation would be critical at 1 $\mu\text{L}/\text{min}$ in a 100- μm i.d. capillary in the case of ES in a magnetic sector instrument, where the sprayer may be at +8 kV or higher. The narrower the internal diameter of the transfer line, the higher the liquid velocity and the smaller is the chance that electrophoretic velocity exceeds the liquid velocity. Inside the barrel of the syringe in the infusion pump, the linear liquid velocity is very low. If the syringe needle is not connected to ground, and if the plunger is pushed forward by a grounded block of metal, a voltage drop exists over the length of the liquid column inside the barrel. Electrophoretic transport of a sample may now take place inside the syringe, as shown schematically in Figure 4. The electric field inside the syringe is eliminated by connecting the syringe needle to ground.

Operation of the electrosprayer at ground potential obviates the reduction of voltage drop in CE/MS and the possibility of electromigration during infusion of a sample. The electric field necessary for the formation of positively charged droplets is generated by floating the inside wall of the ion source at negative high voltage. Ions are drawn toward the opposing wall. To accelerate ions into a mass analyzer inside the vacuum system, a more negative potential has to be applied, which would lead to a very unpractical arrangement of negative high voltages. An elegant system that eliminates the need for acceleration of positive ions toward negative high voltage is the glass capillary for the transportation of ions from the atmospheric-pressure spray region into the vacuum of the mass

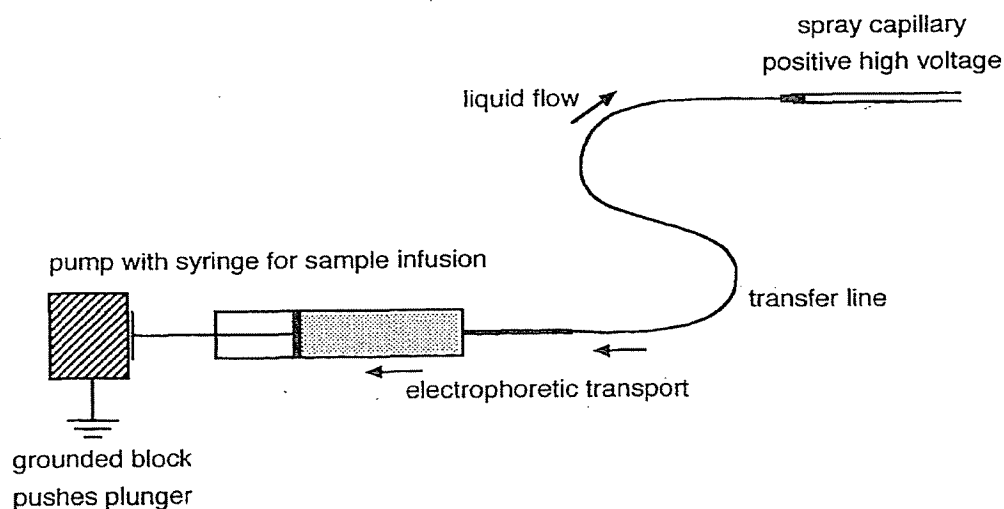


Figure 4. Possibility of electromigration of positively charged sample ions against liquid flow.

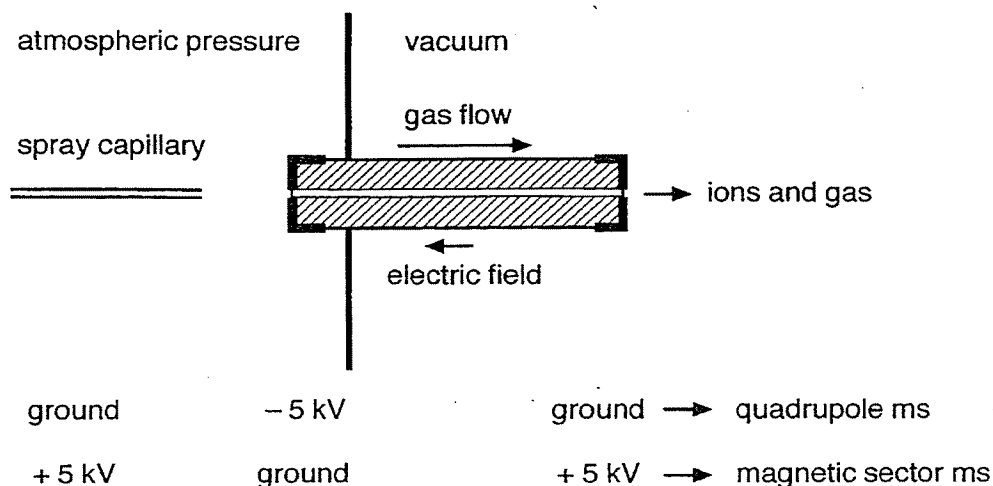


Figure 5. Voltage arrangements for ES capillary and source; isolation between source end plate and accelerating voltage by a glass capillary for ion transport.

spectrometer (see Fig. 5) (14). Ions generated in the atmospheric pressure region of the source either by ES or by atmospheric pressure chemical ionization are drawn into the vacuum region via a glass tube that is metallized at both ends. The linear velocity of the gas flow in the tube is high enough to drag ions into the vacuum even if the inlet of the tube is at a negative high voltage and the outlet is at ground potential. The grounded outlet now serves as a source of ions that can easily be focused into a quadrupole mass analyzer. The atmospheric pressure source and ion optics plus mass analyzer are electrically isolated from one another, which is particularly attractive for magnetic sector instruments. Now the outlet end of the glass capillary is at the accelerating potential of the mass spectrometer, but there is no need to have the spray chamber and the spray capillary at increasingly high voltages. In practice there is a limit to the voltage difference between inlet and outlet of the glass capillary. Apparently, it is not feasible to have the inlet at -5 kV and the spray capillary at ground, as is done in quadrupole instruments. Magnetic sector instruments that incorporate a glass capillary have the spray chamber and capillary inlet at ground, while the spray capillary is held at $+5$ kV, as shown in Figure 5 (15,16).

B. Electrospray and Electrical Discharge

Corona discharge between the ES capillary and its counterelectrode drastically changes the appearance of the mass spectrum. Without a discharge, the spectrum represents ions present in the solution that is dispersed into charged droplets. When a discharge takes place, the spectrum represents the products of ion molecule reactions, as is the case in atmospheric-pressure chemical ionization. At the same time, many ions present in solution can no longer be observed (13). A distinction must be made here between sample ions that exist only as ions in solution, such as quaternary ammonium ions, and ions that can be formed in